DOI: 10.21134/a92j4393

CYTEF XII Congreso Ibérico y X Congreso Iberoamericano de Ciencias y Técnicas del Frio
Universidad Miguel Hernández de Elche
26-06 28-06/2024
UNIVERSITAS Miguel Hernández

ANALYSIS OF SUITABLE METHODOLOGIES FOR COMPRESSOR MASS FLOW RATE CORRECTION TO OTHER SUPERHEAT LEVELS AND REFRIGERANTS

Javier Marchante-Avellaneda[1]*, Rubén Ossorio[1], Emilio Navarro-Peris[1] and Som S. Shrestha[2]

1: Instituto Universitario de Investigación en Ingeniería Energética, Universitat Politècnica de València.
Camí de Vera s/n 46022, Valencia, Spain.
e-mail: jamarav@iie.upv.es
2: Buildings and Transportation Science Division, Oak Ridge National Laboratory.
Oak Ridge, TN 37831-6070, USA

Abstract: *This paper investigates the impact of suction conditions and refrigerant on scroll compressor mass flow rate by using calorimeter tests from AHRI-11 and AHRI-21 reports, published by AHRI's Low-GWP Alternative Refrigerants Evaluation program. Two Copeland scroll compressors (20 and 51 cm3) have been analyzed including different suction conditions (SH = 11K, SH = 22K, T_i = 18ºC) and several refrigerants (R134a, R32, R410A, R404A, etc.). Previous studies have explored response surfaces for energy consumption and mass flow rate variables. This study aims to expand the analysis by identifying the optimal approach to extrapolate mass flow rate from specific suction conditions to others SH or suction temperature levels and refrigerants. The current compressor characterization standard relies on the 1981 Dabiri correlation to correct compressor mass flow rate with suction conditions. Thus, this study aims to assess the adequacy of this correction and explore alternative correction methods for improved results.*

Keywords: Compressor Performance, Mass flow rate, Superheat, Suction Temperature, Extrapolation capability

1. INTRODUCTION

Simulation and modeling software have become indispensable for enhancing product quality in contemporary engineering. In the field of heat pumps (HP), they are essential to reduce costs and time during the design stage, providing researchers and manufacturers with powerful tools to assist them in optimizing and designing new units. Different heat pump simulation software has been developed over the years, such as [1,2].

They facilitate effective analysis of HP component substitutions, offering direct feedback for new designs. Moreover, simulation and modeling can substantially reduce development costs by minimizing the requirement for expensive prototypes and experimental campaigns. A comprehensive heat pump model requires detailed component descriptions, typically derived from manufacturer catalog data. Compressor modeling holds particular significance in unit design and optimization as its performance and efficiency greatly influence the overall system performance in HPs. Over the years, compressor modeling has received considerable attention, and several authors have proposed different approaches, including theoretical, semi-empirical, and empirical models. Nowadays, empirical modeling prevails due to its higher accuracy if sufficient experimental data is available [3], where AHRI polynomials [4] are recognized as the predominant method. However, a notable limitation of this approach is that model coefficients are calibrated at specific suction conditions and refrigerant, where model recalibration or corrections are required to predict other suction conditions and fluids.

While suction superheat (SH) minimally affects energy consumption, it significantly impacts mass flow rate prediction. The widely adopted correction was proposed in 1981 by Dabiri and Rice [5] and also included in the compressor characterization standard (AHRI-540 [3]). It includes a simple linear model based on a ratio of densities between the "*calibrated/mapped*" and "*new*" suction conditions and a single correction coefficient. The value reported by the authors for this coefficient was 0.75 based on Jacobs' experimental data [6]. However, no correction exists for extrapolating results to other refrigerants, where dimensionless parameters like volumetric efficiency are often employed.

Given the considerable time since Dabiri's original study, this work aims to analyze in detail whether this correction is still adequate to extrapolate to other suction conditions and evaluate other extrapolation strategies, including extrapolation to other refrigerants. Furthermore, some discrepancies between the original study and the AHRI-540 standard were also analyzed. Dabiri defined this correction based on the density ratio at the compressor's internal suction port, considering an estimated internal superheat, while the standard omits this step directly using the density ratio at inlet shell conditions. Experimental data from multiple sources, including the "Low-GWP Alternative Refrigerants Evaluation Program", are examined to conduct this analysis.

2. METHODOLOGY

Data from the AHRI Low-GWP AREP project have been analyzed in this work, comprising three datasets from two fixed-speed scroll compressors and including different suction conditions and refrigerants [7,8].

Additionally, the datasets from [6,9] were examined to validate assumptions made in Dabiri's original work (Table 1). The study is divided into three sections: Evaluation of Dabiri correlation including the value for the correction factor, proposal of three modeling approaches using SH=11K data for each refrigerant as reference conditions and extrapolating to other suction conditions, and revaluation of proposed models adjusted at SH=11K and reference refrigerant data to extrapolate to other refrigerants and suction conditions. Refrigerant properties were calculated from Refprop [10], and R software [11] was used for statistical analysis. Model performance was evaluated with the error metrics: Maximum Relative Error (MRE), Root Mean Square Error (RMSE), and Coefficient of Variation of RMSE (CV_{RMSE}).

Table 1. Experimental dataset

Source	Type	Model (Manufacturer)	Disp(freq.) cm3(Hz)	Refrigerants tested[a]	Test points	Conditions by refrigerant test
AHRI 21	Scroll	ZS21KAE-PFV (Copeland)	50.96 (60)	R404A[b]/ARM31a/D2Y65/L40 /(R32+R134a)	191/186/183 /173/133	SH=11.11K SH=22.22K
AHRI 11	Scroll	ZP21K5E-PFV (Copeland)	20.32 (60)	R410A[b]/R32/DR5/L41a	196/166/189 /186	T_i=18.33ºC
Winandy 2002	Scroll	-	174 (50)	R22	28	T_i=25ºC
Jacobs 1976	Reciproc.	-	-	R22	2	T_i=18.33ºC

[a]New mixtures composition in [7,8] ; [b]Reference refrigerant;

3. IMPACT OF SUPERHEAT LEVEL AND REFRIGERANT ON MASS FLOW RATE

The mass flow rate of a compressor is notably influenced by suction conditions, particularly the refrigerant density at the compressor inlet. At a designated operating point with defined parameters like swept volume, motor speed, and refrigerant type, the mass flow rate is fixed by the evaporating temperature and superheat level and also influenced by volumetric efficiency depending on the pressure ratio (1).

$$\dot{m} = \rho V_s N \eta_v \quad (1)$$

A common method for accurately modeling compressors' mass flow is through empirical map-based models like the AHRI polynomials. However, such empirical approaches are limited by model fitting to specific suction conditions and refrigerant fluid. While this does not typically affect energy predictions, which tend to remain constant with superheat changes, predicting mass flow rate under different suction conditions requires correction using Dabiri's correlation (2), as provided in the compressor characterization standard.

$$\dot{m}_{new} = \dot{m}_{map} \cdot \left[1 + F \cdot \left(\frac{\rho_{new}}{\rho_{map}} - 1\right)\right] \quad (2)$$

The original F factor, reported as 0.75 by the author, was derived from Jacobs' experiments [6] to correct the variation of volumetric efficiency evaluated at "internal port conditions" with the internal SH. So, Equation (2) initially used density ratios at "internal port conditions" (subindex p) instead of conventional "inlet shell conditions" (subindex i), but the latter is the most widespread form in use today. It is well known that the refrigerant entering the inlet compressor shell at a certain SH level undergoes additional superheat before reaching the internal suction port. Cooling motor windings, internal friction, and heat transfer in discharge and suction manifolds contribute to this internal superheat, reducing refrigerant density compared to inlet shell conditions and increasing temperature by 10ºC to 30ºC or higher in designs, preventing liquid slugging [12].

As originally reported in [5], let's simplify by assuming constant refrigerant pressure (P_e) and specific heat (c_p) from inlet shell to internal port conditions. Thus, Equation (3) governs suction heat transfer:

$$\dot{Q}_{i,p} = \dot{m} c_p \left(T_p - T_i\right) = \dot{m} \Delta h_{i,p} \quad (3)$$

So, if an estimate of $\Delta h_{i,p}$ (enthalpy: $h_p - h_i$) is available, the temperature at the internal port (T_p) could be calculated with Equation (4), where the temperature at the inlet shell is known (T_i).

$$T_p = T_i + \frac{\Delta h_{i,p}}{c_p} = T_i + SH_{i,p} \quad (4)$$

Based on the experimental results of Jacobs, it was assumed in [5], as a simplification, that $\Delta h_{i,p}$ remains constant with a value of 21 kJ/kg. While this assumption has been checked from Jacobs' data, it should be reevaluated with more experimental tests because Jacobs only reported two experimental points. Thus, this study aims to reevaluate this assumption by analyzing the data reported in [9], which includes 28 experimental points with temperature and pressure measurements at both inlet shell and internal port conditions.

As mentioned in the introduction, Dabiri's correction is applied by directly estimating the density ratio at inlet shell conditions. Both approaches — considering inlet shell conditions and inlet port conditions — will also be evaluated in this study. In order to simplify this analysis, suitable expressions will be derived by incorporating the real gas equation and Equation (4). In this way, the mass flow rate can be estimated according to inlet shell conditions — Equation (5) — or inlet port conditions — Equation (6) —, as outlined below:

$$\dot{m} = \frac{V_s N}{\frac{R_u}{M} Z_i} \cdot \frac{1}{T_i} \cdot P_e \cdot \eta_{v,i} \quad (5) \qquad \dot{m} = \frac{V_s N}{\frac{R_u}{M} Z_p} \cdot \frac{1}{T_p} \cdot P_e \cdot \eta_{v,p} \quad (6)$$

Therefore, two volumetric efficiencies can be defined: $\eta_{v,i}$ and $\eta_{v,p}$, evaluated at inlet shell and internal port conditions. This gives us a suitable formulation that will also facilitate the analysis when also evaluating extrapolation to other refrigerants, as it includes their properties: molar mass (M), compressibility factor (Z_p and Z_i), and specific heat at constant pressure (c_p).

The following subsection will assess the experimental data reported in [9] to analyze the evolution of $\Delta h_{i,p}$ at different operating points. The evolution of $\eta_{v,i}$, and $\eta_{v,p}$ will also be evaluated to understand how the internal superheat affects the volumetric efficiency and to determine if there is any advantage in approximating the density ratio at internal port conditions.

3.1. Internal superheat and volumetric efficiencies at both inlet shell and internal port conditions

This section analyzes the dataset reported in [9] to evaluate Dabiri's assumptions. The dataset comprises 27 tests of a hermetic scroll compressor equipped with internal sensors and operating at a constant inlet shell

temperature of 25ºC. These measurements allow us to calculate refrigerant conditions at the internal suction port and the inlet shell, allowing for the calculation of $\Delta h_{i,p}$. In this database, $\Delta h_{i,p}$ varies from 6.7 to 21.8 kJ/kg, with an average value of 13.5 kJ/kg. Further analysis reveals a correlation of $\Delta h_{i,p}$ with the enthalpy difference between discharge and suction ($\Delta h_{i,2}$). This relationship is logical, as higher $\Delta h_{i,2}$ indicates longer compression and higher discharge temperatures, resulting in higher internal superheat. This dependency is represented in Figure 1-left.

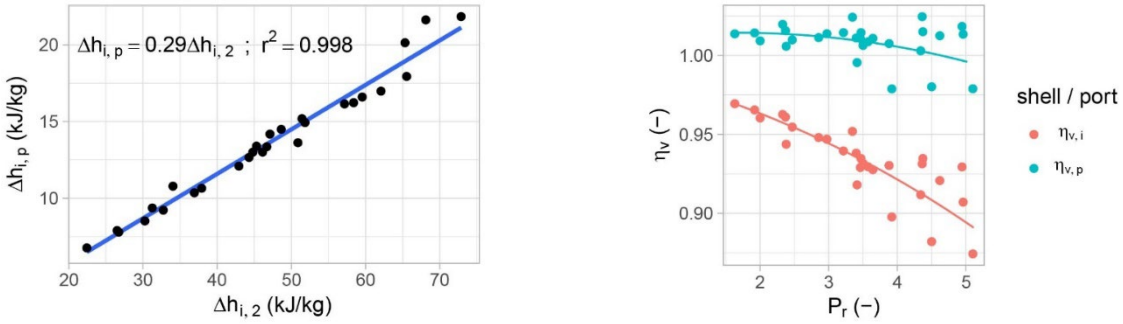

Figure 1. $\Delta h_{i,p}$ vs $\Delta h_{1,2}$ (left-hand) and η_v at shell inlet and internal port conditions vs P_r (right-hand)

This relationship but selecting isentropic discharge conditions ($\Delta h_{i,2s}$) has also been evaluated, where although with slightly more spread in the data, allows us to estimate $\Delta h_{i,p}$ as a certain percentage of $\Delta h_{i,2s}$. In this case, the regression adjustment obtains a higher value for the adjustment factor (0.4) and a slightly lower r^2 (0.994). The dataset reported in [9] includes an additional point with the same conditions tested by Jacobs but with a different value for $\Delta h_{i,p}$ (12.6 kJ/kg). This suggests that $\Delta h_{i,p}$ may change with compressor size, design, and refrigerant. So, assuming a constant $\Delta h_{i,p}$ as supposed in [5] is inappropriate; estimating it as a certain percentage of $\Delta h_{i,2s}$ is more suitable. Concerning the volumetric efficiencies estimated at inlet shell and port conditions ($\eta_{v,i}$ and $\eta_{v,p}$), Figure 1-right shows its evolution with pressure ratio (P_r). $\eta_{v,i}$ shows a nearly linear trend P_r, commonly used for mass flow rate characterization. $\eta_{v,p}$ shows less change with P_r, suggesting a constant or quadratic dependence may be more appropriate. These considerations may be specific to scroll compressors, as the analyzed data exclusively involves this technology.

4. PROPOSED MODELS

Three scenarios will assess mass flow extrapolation to diverse suction conditions and refrigerants using AHRI 21 and 11 data. First, the mean F-factor from Dabiri's correlation (8) will be determined and it will be adjusted using all suction conditions for each refrigerant and a superheat of 11K as map conditions. This will be compared with the original value reported in [5], considering density ratios at inlet shell and internal port conditions and assuming a constant $\Delta h_{i,p}$ of 21 kJ/kg for inlet port conditions. Then, three approaches will be analyzed: **Case A**: Similar to AHRI polynomials (7), fitted for each refrigerant at SH=11K. Equation (8) corrects to other suction conditions. After that, extrapolation to different refrigerants is applied by applying an additional correction based on the density ratio between the new refrigerant and the base refrigerant. **Case B**: Adopts conventional volumetric efficiency, (9) and (10), based on pressure ratio, with refrigerant properties at inlet shell conditions. **Case C**: Like Case B, it evaluates refrigerant conditions at the internal port. A two-step adjustment method based on the trends observed in the previous section is proposed: iteratively adjust k-factor (11) considering constant volumetric efficiency at inlet port conditions. Then, port conditions are calculated using the estimated k-factor, and Equation (12) is adjusted. Equation (11) with real discharge conditions will also be considered to quantify the precision loss when estimating $\Delta h_{i,p}$ under isentropic discharge conditions.

A:
$$\dot{m}_{map} = k_0 + k_1 P_e + k_2 P_c + k_3 P_e P_c \quad (7)$$
$$\dot{m}_{new} = \dot{m}_{map} \cdot \left[1 + F \cdot \left(\frac{\rho_{new}}{\rho_{map}} - 1\right)\right] \quad (8)$$

B:
$$\dot{m} = \frac{V_s N}{\frac{R_u}{M} Z_i} \cdot \frac{1}{T_i} \cdot P_e \cdot \eta_{v,i} \quad (9)$$
$$\eta_{v,i} = k_0 + k_1 P_r + k_2 P_r^2 \quad (10)$$

C:
$$\dot{m} = \frac{V_s N}{\frac{R_u}{M} Z_p} \cdot \frac{1}{T_i + k \cdot \frac{(h_{2s} - h_i)}{c_{p,i}}} \cdot P_e \cdot \eta_{v,p} \quad (11)$$
$$\eta_{v,p} = k_0 + k_1 P_r + k_2 P_r^2 \quad (12)$$

5. ANALYSIS OF RESULTS

The results of case A, B and C approaches are summarized below. Due to space constraints, only prediction errors are presented in Tables 2 and 3. First, Table 2 shows the mean values for the F-factor by using all suction conditions for each refrigerant and estimating the density ratios at inlet shell/port conditions. Low prediction errors were observed regardless of the density ratio used (inlet shell or port conditions), ranging between 0.4-1.3% of CV_{RMSE}. The original F coefficient of 0.75 is found suitable but selecting the density ratios at inlet shell instead of at inlet port. The estimation of the ratio of densities to inlet port by using a constant $\Delta h_{i,p}$ as established in [5] did not improve the results, including a higher mean value for F of 0.833. So, the original F coefficient of 0.75 will be adopted for Case A, with the density ratio estimated at inlet shell conditions.

Table 2. F-factor adjustment. Density ratio at inlet shell and port conditions. SH=11K selected as map conditions

ρ at inlet shell			ρ at inlet port: $\Delta h_{i,p} = 21$kJ/kg			Fluid	Report
F	CV_{RMSE} (%) (RMSE (kg/h))	MRE (%)	F	CV_{RMSE} (%) (RMSE (kg/h))	MRE (%)		
0.863	0.431 (0.489)	1.349	0.975	0.435 (0.494)	1.351	R410A	AHRI 11
0.789	1.015 (0.825)	3.259	0.862	1.010 (0.821)	3.227	R32	
0.657	1.100 (0.974)	3.974	0.735	1.099 (0.972)	3.977	DR5	
0.429	1.339 (1.077)	3.475	0.480	1.338 (1.075)	3.468	L41a	
0.862	0.286 (0.554)	0.931	1.013	0.295 (0.570)	1.009	R404A	AHRI 21
0.734	0.222 (0.277)	0.856	0.850	0.222 (0.277)	0.858	ARM31a	
0.750	0.360 (0.495)	1.640	0.865	0.359 (0.493)	1.634	D2Y65	
0.755	0.511 (0.569)	1.662	0.863	0.509 (0.567)	1.638	L40	
0.759	0.502 (0.593)	1.846	0.861	0.496 (0.586)	1.826	R32+R134a	

With a determined mean value for the F coefficient set at 0.75, we proceeded to evaluate approaches A, B, and C. Initially, the extrapolation capability was assessed for each method to extrapolate to other suction conditions. Table 3 shows the prediction errors for cases A, B, and C, with models fitted at 11K superheat for each refrigerant. Furthermore, in case C, we have included results considering real discharge conditions in Equation (11). While real discharge conditions cannot be integrated as a variable in the model, this case is presented to compare them with the prediction of case C under isentropic discharge conditions.

Table 3. Summary of errors in cases A, B and C. SH=11K selected as map conditions

Case A	Case B	Case C ($\Delta h_{i,2s}$)		Case C ($\Delta h_{i,2}$)		Fluid	Report
F	CV_{RMSE} (%) MRE (%)	CV_{RMSE} (%) MRE (%)	k_{2s}	CV_{RMSE} (%) MRE (%)	k_2	CV_{RMSE} (%) MRE (%)		
0.75	0.86 (1.99)	1.02 (2.25)	1.19	0.83 (2.13)	0.74	0.41 (0.99)	R410A	AHRI 11
0.75	1.06 (2.80)	1.44 (2.86)	1.01	1.37 (3.80)	0.73	0.69 (1.67)	R32	
0.75	1.11 (4.30)	1.94 (6.13)	1.05	1.65 (6.64)	0.71	1.03 (4.49)	DR5	
0.75	1.53 (3.93)	2.77 (5.92)	1.03	2.25 (5.58)	0.71	1.41 (3.01)	L41a	
0.75	0.77 (1.94)	0.90 (2.54)	0.71	0.61 (1.78)	0.36	0.45 (1.20)	R404A	AHRI 21
0.75	0.26 (1.04)	1.67 (3.28)	0.63	1.14 (2.68)	0.36	0.65 (1.22)	ARM31a	
0.75	0.29 (1.27)	1.57 (3.10)	0.56	1.17 (2.53)	0.31	0.81 (1.62)	D2Y65	
0.75	0.51 (1.48)	1.52 (2.83)	0.55	1.01 (2.34)	0.35	0.56 (1.37)	L40	
0.75	0.61 (1.78)	1.36 (3.29)	0.72	1.01 (2.78)	0.43	0.60 (2.01)	R32+R134a	

Comparing Cases A, B, and C indicates lower prediction errors in Case C selecting real discharge conditions. Consistent k-values are observed across compressor types: 0.7 for the 20 cm^3 compressor and 0.35 for the 51 cm^3 compressor. While internal SH estimation without internal port measurements cannot be verified, the low prediction errors suggest a reliable estimate. A higher k-value for the smaller compressor is logical due to increased heat transfer. In a common scenario with unknown discharge conditions, using isentropic discharge conditions (Case C, $\Delta h_{i,2s}$) obtains higher k-values and prediction errors similar to cases A and B. So, estimating internal superheat based on $\Delta h_{i,2s}$ does not improve results. However, Figure 2 shows cases A, B, and C, fitted to the reference refrigerant at SH=11K and extrapolating to all suction conditions and refrigerants. Refrigerant L41a was excluded after reporting an unjustified loss of volumetric efficiency compared to other mixtures of similar composition. In this case, approach C shows lower prediction errors even assuming isentropic conditions at discharge, suggesting a promising model when extrapolation to other fluids is required.

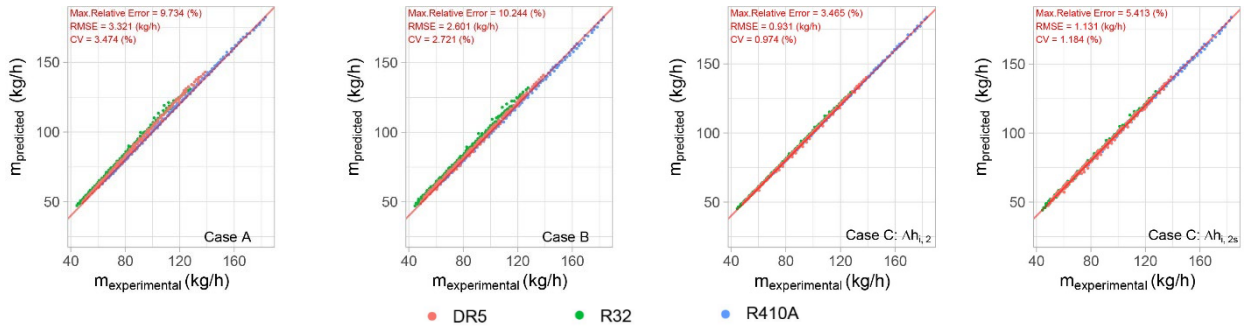

Figure 2. AHRI 11: R410A SH=11K as reference. Extrapolation to other refrigerants and suction conditions

6. CONCLUSIONS

A thorough investigation reveals the following key findings:

1. Map-based models effectively predict energy consumption, but mass flow rate predictions require correction for other suction conditions.
2. Dabiri correlation is commonly used for such corrections, with a corrector factor typically set at 0.75.
3. The analyzed data indicates the unsuitability of assuming a constant $\Delta h_{i,p}$ and reveals that — in scroll compressors — volumetric efficiency evaluated at inlet port remains almost constant at moderate P_r.
4. 0.75 is a suitable value for the Dabiri's F-factor considering the density ratio at inlet shell conditions.
5. Three modeling approaches were evaluated, with Case A (selecting the Dabiri correction) proving most effective for extrapolating to other suction conditions with the same refrigerant.
6. Case C, incorporating internal superheat estimation and volumetric efficiency at inlet port conditions, yielded better results when extrapolating to different refrigerants.

ACKNOWLEDGEMENT

This work was supported by the "Ministerio de Ciencia e Innovación" (PID2020-115665RB-I00) and Universitat Politècnica de València (PAID-10-23). Resources at Oak Ridge National Laboratory were utilized. Thanks to the late Dr. José Miguel Corberán, without whom this work wouldn't have been possible. Dr. José Miguel Corberán passed away in July 2022. My heartfelt support to his family. I hope we did you proud.

REFERENCES

[1] Thermal Area IUIIE, IMST-ART: A simulation tool to assist the selection, design and optimization of refrigeration equipments and components, IMST-GROUP, Instituto de Ingeniería Energética, UPV.
[2] J. Brown, R. Brignoli, P. Domanski, Y. Yoon, CYCLE_D-HX: NIST vapor compression cycle model accounting for refrigerant thermodynamic and transport properties; version 2, user's guide, (2021).
[3] H. Cheung, S. Wang, A comparison of the effect of empirical and physical modeling approaches to extrapolation capability of compressor models by uncertainty analysis: A case study with common semi-empirical compressor mass flow rate models, International Journal of Refrigeration 86 (2018) 331–343.
[4] AHRI, AHRI-540. Performance Rating of Positive Displacement Refrigerant Compressors, (2020).
[5] A.E. Dabiri, C.K. Rice, Compressor-simulation model with corrections for the level of suction gas superheat, Oak Ridge National Lab., TN (USA); Science Applications, Inc., La Jolla, CA (USA), 1981.
[6] J. Jacobs, Analytic and Experimental Techniques for Evaluating Compressor Performance Losses, International Compressor Engineering Conference (1976).
[7] S. Shrestha, I. Mahderekal, V. Sharma, O. Abdelaziz, TEST REPORT #11. Compressor calorimeter test of R-410A alternatives R-32, DR-5, and L-41a, Oak Ridge National Laboratory, 2013.
[8] S. Shrestha, V. Sharma, O. Abdelaziz, TEST REPORT #21. Compressor calorimeter test of R-404A alternatives ARM-31a, D2Y-65, L-40, and R-32/R-134a (50/50), Oak Ridge National Laboratory, 2013.
[9] E. Winandy, C.S. O, J. Lebrun, Experimental analysis and simplified modelling of a hermetic scroll refrigeration compressor, Applied Thermal Engineering 22 (2002) 107–120.
[10] E.W. Lemmon, I.H. Bell, M.L. Huber, M.O. McLinden, NIST Standard Reference Database 23: Reference Fluid Thermodynamic and Transport Properties-REFPROP, Version 10.0.
[11] R Core Team, R: A Language and Environment for Statistical Computing, (2023).
[12] C.C. Hiller, L.R. Glicksman, Improving heat pump performance via compressor capacity control: analysis and test, MIT Energy Lab, 1976.